Journal of Cultural Heritage 40 (2019) 265–273

Available online at
ScienceDirect
www.sciencedirect.com

Elsevier Masson France
EM|consulte
www.em-consulte.com/en

Pompeii special issue

Mineralogical clustering of the structural mortars from the Sarno Baths, Pompeii: A tool to interpret construction techniques and relative chronologies

Michele Secco[a,b,*], Caterina Previato[c], Anna Addis[d], Giulia Zago[b], Angelique Kamsteeg[a], Simone Dilaria[c], Caterina Canovaro[d], Gilberto Artioli[b,d], Jacopo Bonetto[c]

[a] University of Padova, Department of Civil, Environmental and Architectural Engineering (ICEA), Italy
[b] University of Padova, Inter-Departmental Research Center for the Study of Cement Materials and Hydraulic Binders (CIRCe), Italy
[c] University of Padova, Department of Cultural Heritage (DBC), Italy
[d] University of Padova, Department of Geosciences, Italy

ARTICLE INFO

Article history:
Received 6 August 2018
Received in revised form 28 February 2019
Accepted 19 April 2019
Available online 30 May 2019

Keywords:
Pompeii
Mortar
Pozzolanic reaction
XRPD quantitative phase analysis
Principal component analysis

ABSTRACT

Structural mortars constitute one of the most diffuse geomaterials, with stones and bricks, in ancient monuments and architectural complexes, especially related to the Roman civilization, which pushed the binder technology to technical levels unsurpassed until post-industrial revolution times. The archaeometric study of mortars is an essential tool to extrapolate great amounts of information concerning supply of raw materials, technological skills of the ancient civilizations and, finally, relative and absolute chronologies of diachronic construction phases, both related to ancient and modern architectural modifications of the buildings. In this contribution, a novel approach for the quantitative mineralogical analysis of ancient mortars is proposed. The analytical process is based on the integrated application of quantitative phase analysis (QPA) of mineral components by means of the Rietveld method applied to X-ray powder diffraction (XRPD) data and multivariate statistical treatment of the obtained results by means of the principal component analysis. The methodology has been applied on a wide set of binding materials sampled from different structural elements of the Sarno Baths, a five-storey building located in the Pompeii archaeological site. The building is characterized by a marked complexity both in terms of structural layout and constructive techniques, being the result of several modifications in ancient times from the Late Republican age up to the Vesuvius eruption in 79 AD. Furthermore, several poorly documented restorations have been performed between the 19th century and the first half of the 20th century AD. In this perspective, a quantitative characterization of the employed mortars resulted useful not only to define ancient constructive technologies and relative chronologies, but also to discriminate between the original and restored parts of the building for the execution of adequate restoration procedures. The statistical clustering of the quantitative XRPD data clearly defined two ancient constructive phases and allowed a precise definition of the structural elements rebuilt in recent times. Furthermore, the obtained results have been cross-checked with additional analyses, namely XRD analyses on the separated binder fractions, petrographic analyses and scanning electron microscopy-energy-dispersive microanalyses. Such multi-analytical approach allowed the detailed characterization of the employed raw materials, of the pozzolanic reactions between binder and aggregate and of the textural and microstructural characteristics of the mortars. The data interpretation yielded interesting insights both on the advanced optimization of mix designs of binding materials in Roman times, to improve the structural properties of the architectural elements according to their functions, and on the formulation of the restoration products during the historic excavations in Pompeii.

Introduction

Decodifying mural stratigraphic sequences of ancient architectural structures has always been one of the crucial aims in archaeological research, owing its enormous potentialities in defining not only the constructive phases of complex buildings, but also

* Corresponding author at: University of Padova, Department of Civil, Environmental and Architectural Engineering (ICEA), Italy.
E-mail address: michele.secco@unipd.it (M. Secco).

https://doi.org/10.1016/j.culher.2019.04.016
1296-2074/

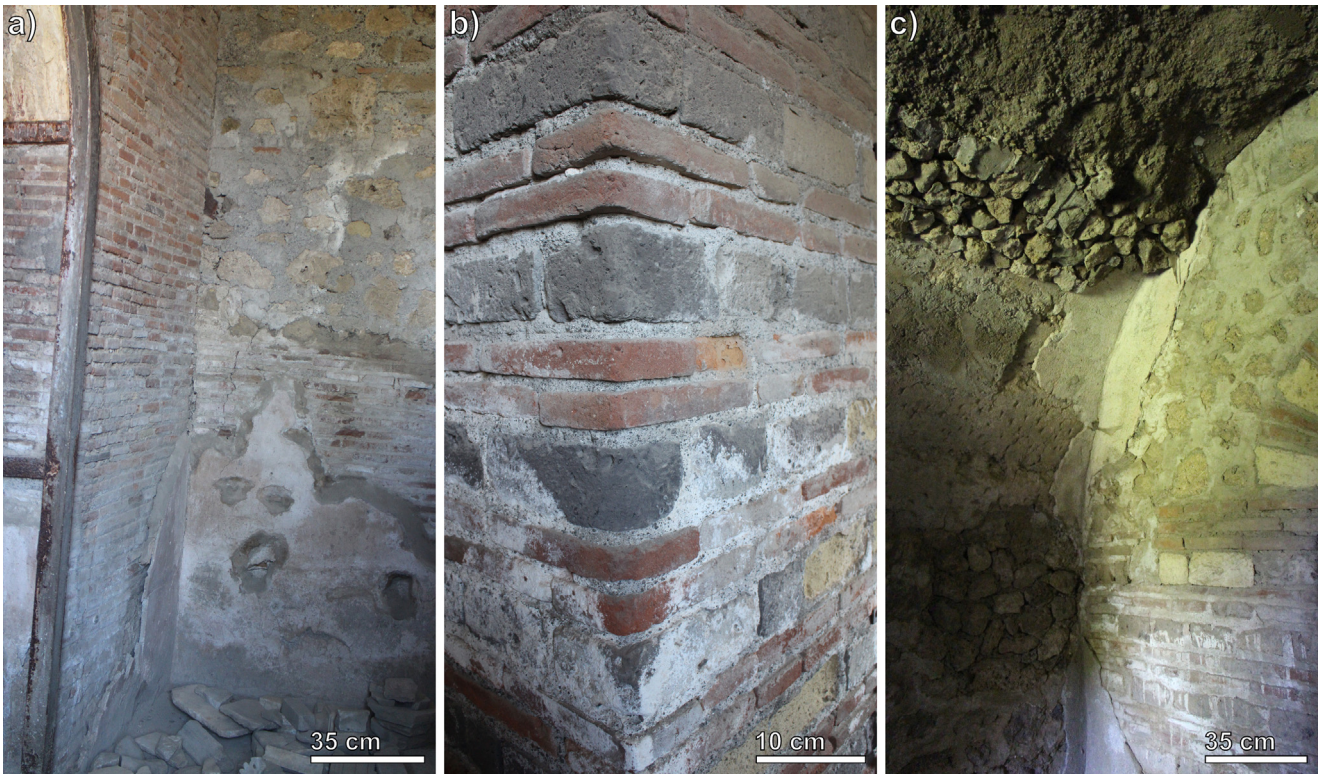

Fig. 1. Examples of the heterogeneous masonry textures of the Sarno Bath complex.

the technological evolution of the construction practices over the entire service life of the structures and beyond.

In this perspective, the contribution of modern archaeometrical research on the analysis of structural binding materials like bedding mortars and concretes proved to be a fundamental weapon for the definition of construction techniques and relative chronologies of ancient architecture. This is mainly due to their widespread utilization in the past, and owing the fact that they generally constitute a univocal compositional proxy for each single construction phase [1].

The potentialities of heritage science in interpreting synchronic and diachronic evolutions of archaeological contexts is proved by several recent studies, employing mainly a mix of petrographic, geochemical and microstructural approaches [2–5]. In these works, the application of mineralogical techniques such X-ray powder diffraction is somewhat limited to qualitative verifications of the textural and chemical outputs. Furthermore, when applied through advanced approaches such as quantitative phase analysis by Rietveld refinement [6] and crystallographic studies [7], the mineralogical characterization of binding materials is partly biased by the low statistical significance, apart from a recent contribution [8] showing the promising potentialities of a mixed mineralogical-statistical approach for the study of archaeological buildings characterized by complex mural stratigraphic sequences.

The Sarno Bath complex in Pompeii (Naples, southern Italy) is a clear example of intricated structural palimpsest generated after numerous and not well-defined architectural modifications both in ancient and modern times.

Situated in the south-western part of Pompeii (*Regio* VIII, *Insula* 2, nos. 17-21), the building stands on the slopes of the city hill, not far from the forum. Due to its position, it has a peculiar plan developed on 5 different levels connected by stairs and tunnels. The façade of the building, heading south, is about 40 meters long, decorated with windows and niches.

According to most of the scholars [9–11], the first building phase of the complex dates back probably to the Late Republican age (2nd century BC): in this period, two different *atrium* houses were built. They were mainly extended on the ground level of the ancient city (level 0), with a probable occurrence of lower rooms (levels −1, −2, −3, −4). At a later stage, another house was built in the triangular space between the two *atria*, together with a bathing complex at level -3. Then, a new apartment was built over the baths. The Sarno Baths were partly destroyed by the earthquake which affected Pompeii in 63 AD, and renovation works were undertaken in various parts of the complex, still in progress during the Vesuvius eruption of 79 AD.

The Sarno Baths remained buried under the pumices until the end of the 19th century, when in few years (1887–1893) the majority of the complex, starting from the upper level, was dug up under the supervision of Antonio Sogliano and August Mau [10]. At that time, the southern façade was almost entirely covered by excavation dumps and only its upper part was visible (level −3), because in previous times the area along the front of the building had been used as a dump. On this occasion, the complex was heavily restored, especially in its inner part [12].

New restoration works were performed starting from the 1930s under the supervision of Amedeo Maiuri [10], when modern stone walls were constructed and iron bars were inserted in the structure to close doorways and windows. Finally, during the early 1950s the dump on the southern side of the building was removed and the southern façade was cleared.

Each of the building phases and activities (ancient and modern) here briefly presented (see [13,14] for a more detailed description) determined modifications both in the layout and in the structural members of the Sarno Bath complex, clearly indicated by the complexity of the masonry textures (Fig. 1). These interventions are very difficult to recognize, also because there is no documentation about the renovation works which took place in the last two centuries.

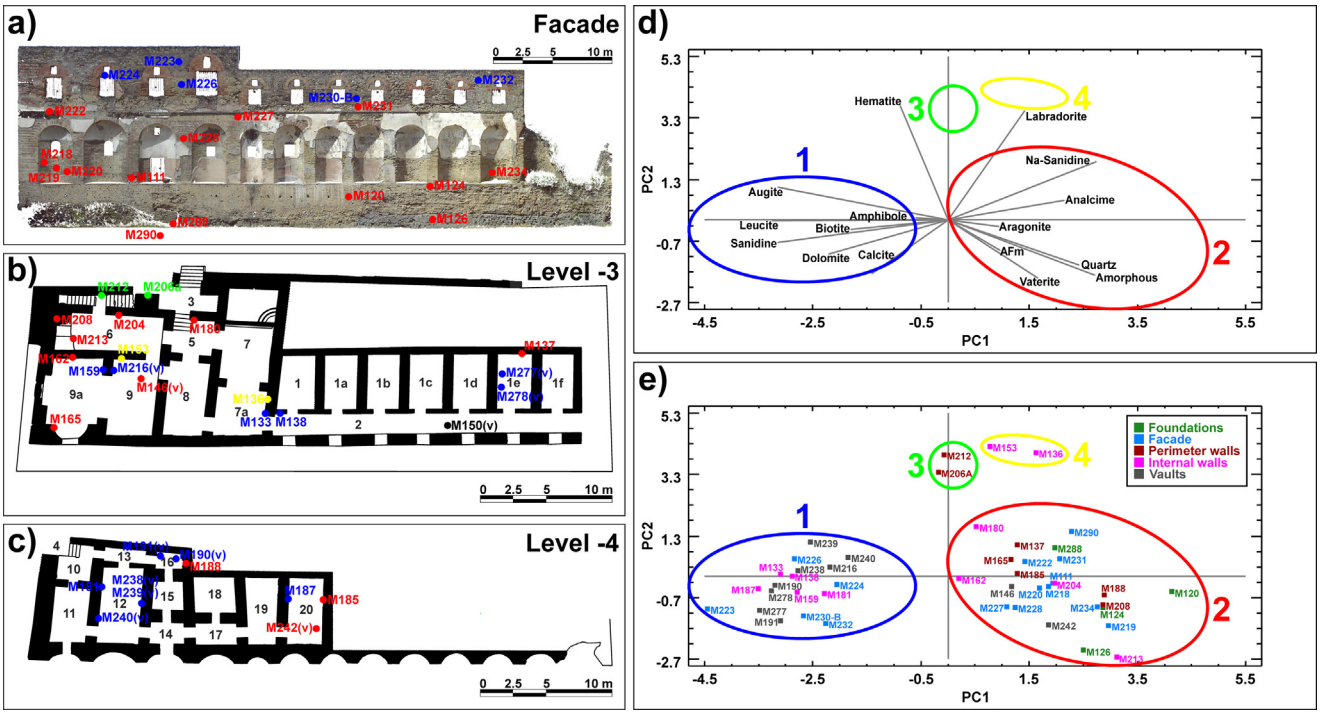

Fig. 2. a, b, c: Plan of the mortar sampling points on the façade (orthophotograph by Achilli et al. [41]) and in the inner levels; d: score plot and e: loading plot of the principal component analysis of the mineralogical quantitative data: the first two components (PC1 and PC2) have been plotted, representing 37% and 14% of the total variance, respectively. The four defined mineralogical groups are indicated by coloured ellipses in the score and loading plots, and the sample names and locations in the maps are coloured according to the mineralogical group of pertinence.

Such architectural complexity is clearly stated by Ioppolo [11], who points out the difficulty in discriminating ancient and modern architectural contributions, also due to the tendency in using the same types of building materials for the masonry units over time [11]. The clue to solve such complex archaeological issue is indicated by Ioppolo itself, stating that ". . .a continuous chemical-mineralogical analysis for each wall portion would be necessary to distinguish such interventions from the original structures" [11].

Starting from the positive outputs obtained in a recent study of evolution of the flooring Vitruvian recipes in the city of Aquileia [15], this work is aimed at employing the multivariate statistical analysis of mortars quantitative mineralogical profiles as a fundamental tool to study construction techniques and relative chronologies of the Sarno Bath complex. The obtained results have been crosschecked through the application of standard petrographic and microstructural characterization techniques.

Materials and methods

The sampling of the structural mortars was preceded by an accurate on-site survey to define the most suitable samples to collect in terms of archaeological and architectural significance. A total number of 47 samples was taken, limiting the area of investigation to the fully preserved levels of the building (level −3 and level −4) and to the external façade and taking into account only structural mortars (bedding mortars and concretes). Samples were removed mechanically with hammers and chisels, paying attention in avoiding external and clearly altered portions, in order to study materials as close as possible to the original conservation state. The full list of analyzed materials is reported in Table S1, together with their position and structural element of pertinence (either perimeter walls, internal walls or vaults). A detailed map with the sample positions is reported in Fig. 2a, 2b, 2c. Sample M290 was collected from a portion of collapsed wall related to level -3 and unearthed during a survey excavation [16], so it can be considered as a reference for the original binding materials.

Mineralogical analyses were performed both on the bulk fragments of mortar (both binder and aggregate) and on selected binder-concentrated samples through X-ray powder diffraction (XRPD). As for the bulk samples, the analyses were carried out after micronization of the materials through a McCrone micronizing mill, using a plastic jar with agate grinding elements and ethanol 99% as micronizing fluid, while the binder-concentrated samples were obtained through the Cryo2Sonic 2.0 separation procedure [17]. Data were collected using a Bragg–Brentano θ-θ diffractometer (PANalytical X'Pert PRO, Cu Kα radiation, 40 kV and 40 mA) equipped with a real time multiple strip (RTMS) detector (PIXcel by Panalytical). Data acquisition was performed by operating a continuous scan in the range 3–85 [°2θ], with a virtual step scan of 0.02 [°2θ]. Diffraction patterns were interpreted with X'Pert HighScore Plus 3.0 software by PANalytical, qualitatively reconstructing mineral profiles of the compounds by comparison with PDF databases from the International Centre for Diffraction Data (ICDD). Then, quantitative phase analysis (QPA) was performed on the sole bulk samples using the Rietveld method [18]. Refinements were accomplished with TOPAS software (version 4.1) by Bruker AXS. The determination of both crystalline and amorphous content was calculated on most samples by means of the internal standard method, with the addition of 20 wt% of zincite to the powders as internal standard. The observed Bragg peaks in the powder patterns have been modelled through a pseudo-Voigt function, fitting the background by a 12 coefficients Chebyshev polynomial. For each phase, the lattice parameters, Lorentzian crystal sizes and scale factors have been refined. Although samples were prepared with the back loading technique to minimize preferred orientation of crystallites *a priori*, during the refinement, any residual preferred orientation effect was modelled with the March Dollase algorithm [19]. The starting structural models for the refinements were taken

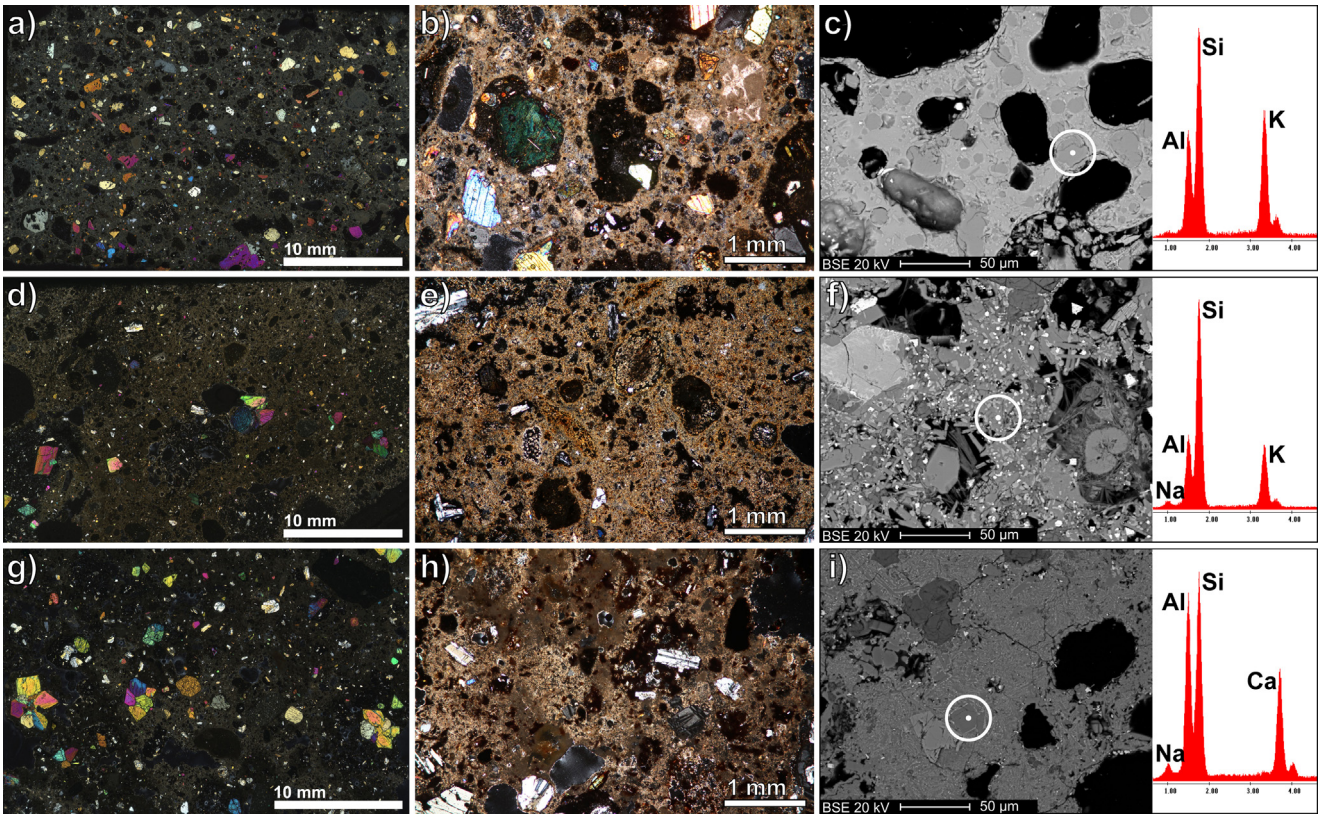

Fig. 3. Petrographic, microstructural and microchemical characteristics of the three main groups of mortars. Group 1: TL-OM micrographs at crossed polars, samples M138 (a) and 187 (b); sample M187, backscattered electrons image (BSI) of a volcanic scoria aggregate particle and EDS microanalysis of a leucite crystal (c). Group 2: TL-OM micrographs at crossed polars, samples M124 (d) and 208 (e); sample 208, BSI of a crystalline volcanic rock aggregate particle and EDS microanalysis of a Na-sanidine crystal (f). Group 2: TL-OM micrographs at crossed polars, samples M124 (d) and 208 (e); sample 208, BSI of a crystalline volcanic rock aggregate particle and EDS microanalysis of a Na-sanidine crystal (f). Group 3: TL-OM micrographs at crossed polars, samples M206A (g) and 212 (h); sample 212, BSI of a tephritic foam lava aggregate particle and EDS microanalysis of a plagioclase crystal (i).

from the International Crystal Structure Database (ICSD). In order to interpret possible reciprocal correlations between the mineralogical profiles of the samples, the quantitative mineralogical data were subjected to multivariate statistical treatment by means of the principal component analysis (PCA). PCA was performed on logtransformed data, using the covariance matrix. All statistical analyses were performed using Statgraphics Centurion XVI software.

The mineralogical data were crosschecked through petrographic analyses, following macroscopic and microstratigraphic analytical procedures for the study of mortar-based building materials described in UNI Norm 11176:2006 "Cultural heritage - Petrographic description of a mortar". The study was performed both on massive portions, through macroscopic and stereomicroscope observations, and by transmitted polarized light optical microscopy (TL-OM) on 30 μm thin sections. Finally, the thin section samples were microstructurally and microchemically characterized by Scanning Electron Microscopy (SEM-EDS). A CamScan MX2500 scanning electron microscope has been used, equipped with a LaB_6 cathode and a four quadrant solid state BSE detector for imaging. The analytical conditions were: accelerating voltage 20 kV; filament current 1.80 A; emission current 20 μA; aperture current 300 nA; working distance 20–30 mm. Furthermore, an EDAX-EDS energy dispersive X-rays fluorescence spectrometer was used for chemical microanalysis, mounting a Sapphire Detector composed by a LEAP + Si(Li) crystal and a Super Ultra Thin Window. Qualitative interpretation of spectra and semiquantitative chemical analysis were performed through SEM Quant Phizaf software.

Results

Mineralogical clustering of the mortars

The quantitative mineralogical profiles of the analyzed mortars (Table S1) highlighted a dominant occurrence of silicate phases for all the samples, namely labradoritic plagioclase, sanidine (both pure and Na-substituted, but never simultaneously present in the same sample), leucite, augite, biotite and analcime, with a sporadic occurrence of amphibole. The clear volcanic origin of such phases indicates the utilization of locally available materials as aggregate fraction [20]. The occurrence of quartz and sporadic dolomite is to be related to limited colluvial contaminations of the aggregate, while hematite is to be related either to the *colluvium* and the volcanic fraction. All the samples are characterized by the occurrence of highly variable amounts of calcite, clearly related to the carbonated calcic binder of the materials. Furthermore, relevant fractions of amorphous compounds are present, related either to glassy components of the volcanic aggregates and to paracrystalline hydrated calcic aluminosilicates, namely C-S-H and AFm phases, formed after pozzolanic reaction between the reactive components of the volcanic aggregates and the lime binder [21]. The occurrence of pozzolanic reaction processes is fully consistent with the use of locally supplied reactive sands [22], renowned since ancient times for their reactive properties [23], and confirmed by the occurrence of crystalline calcium monocarboaluminate AFm phase in several samples [24]. Also, the presence of metastable calcium carbonate polymorphs (vaterite and aragonite) is a further indication of pozzolanic reaction, being reported as common alteration products of

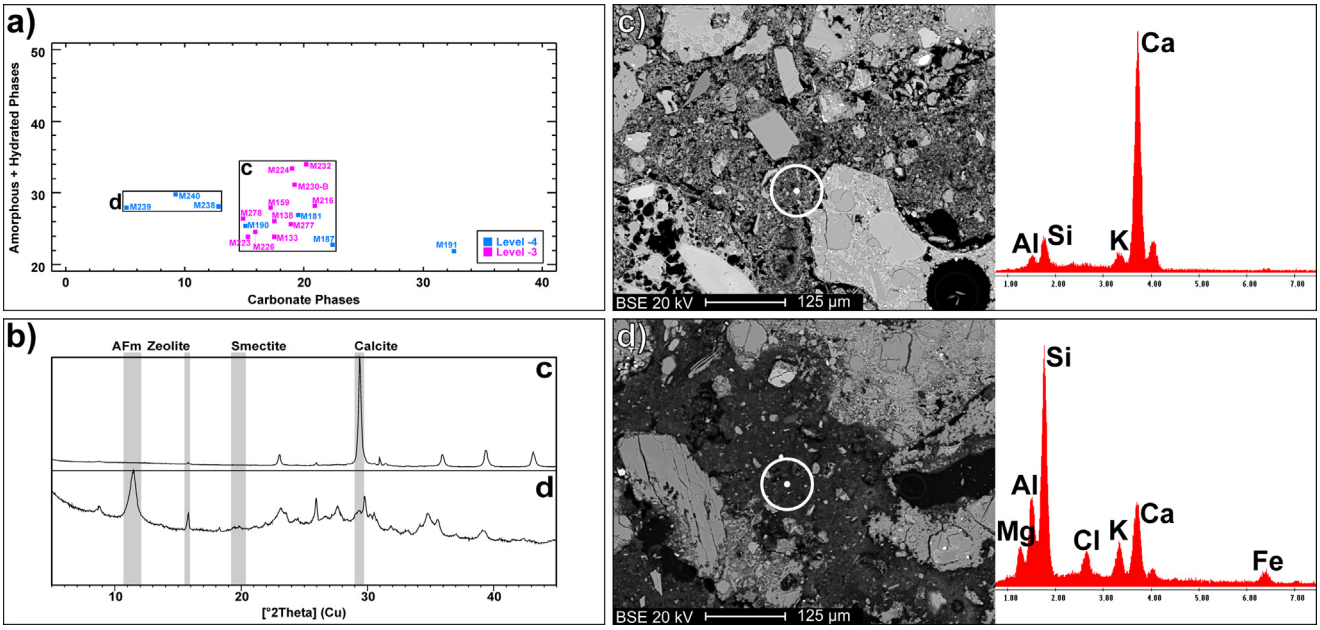

Fig. 4. Mineralogical properties of the binding matrices of group 1 mortars; a: Scatterplot of carbonate vs. amorphous and hydrated phases from the bulk XRPD QPA's; b: XRPD analyses of the binder fractions, samples M133 (c) and M240 (d); c: Sample M133, BSI and EDS microanalysis of the binder matrix; d: Sample M240, BSI and EDS microanalysis of the binder matrix.

C-S-H cementitious binders in hydraulic mortars [25]. Concerning the binder phases, sample M150 is characterized by the occurrence of detectable aliquots of tricalcium silicate C_3S and dicalcium silicate C_2S, common constituents of modern Portland cement-based binders [26]: this is a clear indication that the structural element related to such sample was made during a recent restoration intervention. Finally, several samples are characterized by the limited occurrence of secondary phases, namely gypsum, syngenite, halite, sylvite and gaylussite, clearly related to alteration process due migration and crystallization of soluble salts [27].

The multivariate statistical treatment of the mineralogical dataset by principal component analysis, performed excluding sample M150 of clear modern origin and recalculating the quantitative profiles excluding the alteration phases, allowed to evaluate the correlations between the primary phases, leading to a clear clustering of the analyzed mortars into four groups (Fig. 2d, 2e).

Group 1 is strongly correlated with the abundance of augite, leucite and sanidine, while the correlation with calcite suggests the occurrence of high amounts of carbonated binder. The analyses by TL-OM and SEM-EDS fully confirmed the mineralogical observations: the aggregate fraction of the materials is entirely constituted by euhedral subangular crystals of clinopyroxene (Fig. 3a), associated with subrounded grains of vesicular volcanic scoria with holohyaline texture (Fig. 3b) and rich in equidimensional euhedral leucite crystals (Fig. 3c). The widespread utilization of such type of aggregate has been already attested in the Pompeii archaeological site, and it is fully consistent with local alluvial and coastal sands [22,28]. Sample M191 is slightly differentiated from the other mortars of the group by the occurrence of millimeter-sized carbonate aggregates.

Group 2 is strongly correlated with the abundance of Na-sanidine, analcime and amorphous fraction. While the cross-correlation between analcime and amorphous phase may suggest a high amount of glassy volcanic aggregate, being zeolites widely attested as secondary alteration products of hypohyaline volcanic rocks [29], the high amorphous concentrations may also be related to a higher incidence of pozzolanic reactions than the samples of the previous group, as attested by the strong correlation between this cluster of samples and AFm phase and calcium carbonate metastable polymorphs. Such hypotheses are strongly corroborated by TL-OM and SEM-EDS analyses: the aggregate is composed of a fine yellowish volcanic ash intimately dispersed in the binding matrix, with abundant vesicular aggregates of hypocrystalline pumice often showing interfacial dissolution features related to pozzolanic reaction processes (Fig. 3d, 3e). Furthermore, it is attested the occurrence of crystalline volcanic rock fragments with trachytic texture rich in Na-sanidine microlites (Fig. 3f). Clinopyroxene crystals are significantly less abundant with respect to the previous group. All these features suggest the use of an aggregate fraction constituted of pumiceous volcanic ash pozzolan quarried from unconsolidated levels of the Neapolitan yellow tuff formation, widely attested as common pozzolanic addition during Roman times [25].

Group 3, constituted by two samples (M206 A, M212), shows strong correlation of with hematite and labradorite: these phases are related to the aggregate fraction, entirely constituted of reddish vesicular phonolitic tephrite grains with hypohyaline texture (Fig. 3g, 3h), rich in hematite microcrystals finely dispersed in the groundmass and large phenocrysts of geminated plagioclases (Fig. 3i), clinopyroxenes and leucite. All these features suggest the utilization of an aggregate fraction obtained after fine comminution of tephritic foam lava fragments quarried from the Civita volcanic formation on which the building lies [20].

Group 4 is constituted by two isolated samples (M136, M153) characterized by an aggregate fraction rich in labradorite and Na-sanidine crystals.

Mineralogical properties of the binding matrices

A first compositional insight on the binding matrices of group 1 mortars is given by the ratios of carbonate vs. amorphous and hydrated phases extrapolated from the bulk mineralogical profiles (Fig. 4a): the majority of the samples lies within a narrow compositional range characterized by concentrations of carbonates between 14 and 22 wt%, suggesting a good standardization of the mix designs for such materials. XRPD analyses on the binder-concentrated samples showed that they are almost exclusively

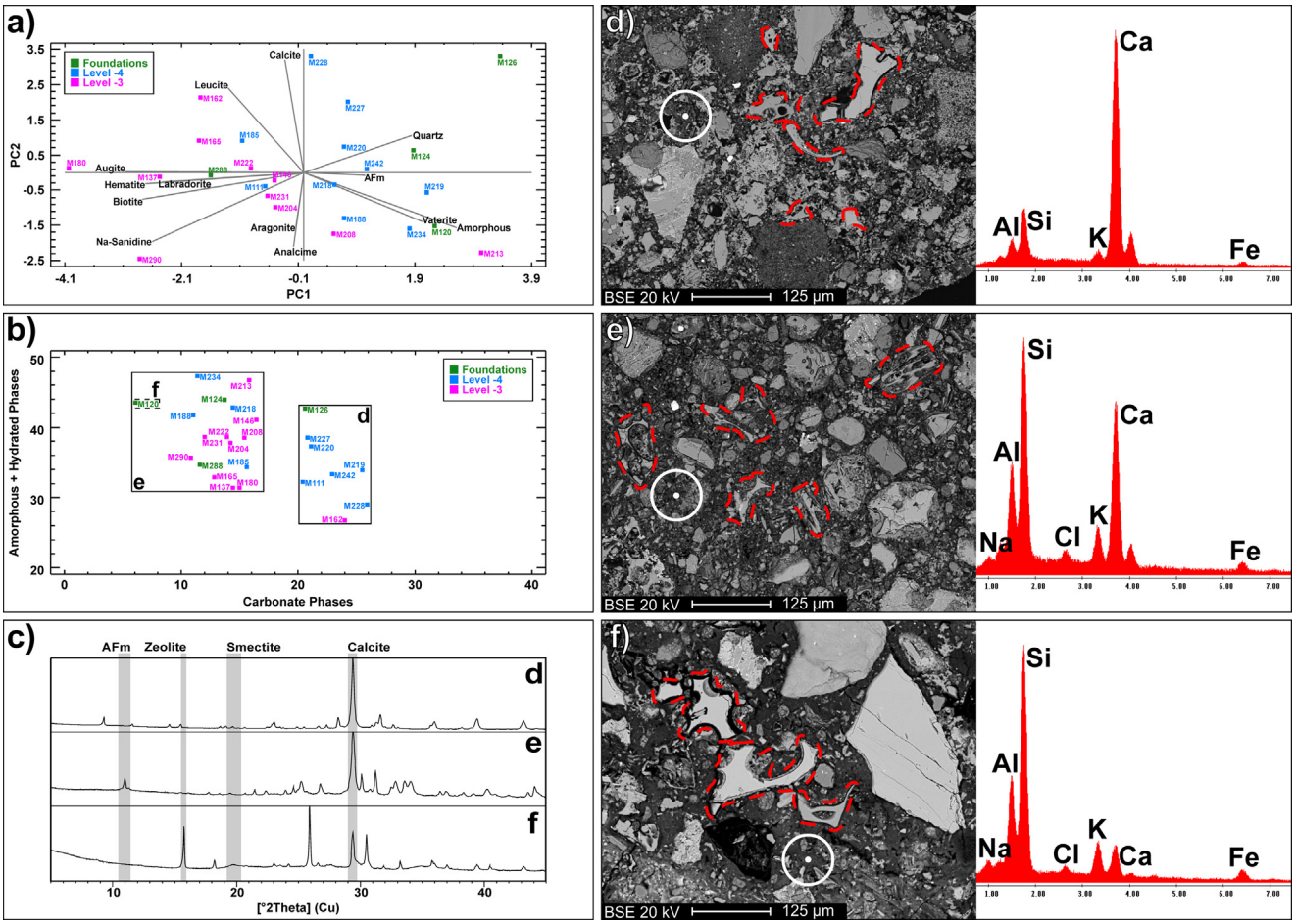

Fig. 5. Mineralogical properties of the binding matrices of group 2 mortars; a: principal component analysis of the mineralogical quantitative data, biplot of the first two components (PC1 and PC2 representing 33% and 17% of the total variance, respectively); b: Scatterplot of carbonate vs. amorphous and hydrated phases from the bulk XRPD QPA's; c: XRPD analyses of the binder fractions, samples M162 (d), M188 (e) and M120 (f); d) Sample M162, BSI and EDS microanalysis of the binder matrix; e) Sample M188, BSI and EDS microanalysis of the binder matrix; f: Sample M120, BSI and EDS microanalysis of the binder matrix.

composed of calcite with a total absence of crystalline pozzolanic phases (Fig. 4b), indicating a low degree of aggregate reactivity. This is further confirmed by SEM-EDS (Fig. 4c), showing the mainly calcic composition of the matrices, with the lack of extensive dissolution features on the volcanic aggregates. The mineralogical differentiation of sample M191, characterized by significantly higher carbonate values, is justified by the occurrence within the mortar of millimeter-sized carbonate aggregates. On the other hand, samples M238, M239 and M240, taken from the vault of room 12, are characterized by remarkably lower calcite content. The XRPD analyses of the binder fractions showed the occurrence of relevant amounts of carbonate-AFm phase, associated with high zeolites and low calcite contents (Fig. 4b): such analytical outputs indicate the addition of fine volcanic ashes to the binding mixture to confer relevant pozzolanic properties, and it is confirmed by SEM-EDS analyses on the binder matrices, showing high silica and alumina values (Fig. 4d).

The principal component analysis on the bulk mineralogical profiles of group 2 mortars highlighted a clustering to positive PC1 values of the samples taken from the −4 level (Fig. 5a). The correlation between positive PC1 values and binder phases, showed by the loading plot, indicates the adoption of higher binder to aggregate ratios for the mortars of the lower level of the building. The plot of the carbonate vs. amorphous and hydrated phases ratios (Fig. 5b) is characterized by a higher dispersion of values with respect to the previous group of samples, suggesting a lower standardization of the mix designs. The materials are clustered within two main groups, a first one characterized by carbonate values over 20 wt%, and a second one with carbonate values lover than 16 wt% and higher amorphous + hydrated phases values. The XRPD analyses on the binder fractions of the first cluster indicate that they are almost exclusively composed of calcite with no pozzolanic phases (Fig. 5c), suggesting a prevalence of aerial reaction by carbonation of lime over pozzolanic reaction. This is confirmed by the SEM-EDS analyses (Fig. 5d), showing both a prevalence of calcic compounds on the matrices, and the occurrence of limited dissolution features on the pumice shards. On the other hand, the binding matrices of the samples related to the second cluster are characterized by the simultaneous occurrence of calcium carbonates and carbonate-AFm phase, as showed by XRPD patterns (Fig. 5c), indicating the mutual triggering of both carbonation and pozzolanic reaction. This is confirmed by SEM-EDS (Fig. 5e), showing both higher silica and alumina values on the matrices than the previous cluster, and relevant dissolution features on the pumice shards. Finally, sample M120 is characterized by low amounts of carbonate phases both in the bulk and binder-concentrated XRPD analysis, with a complete lack of crystalline pozzolanic phases and high amounts of zeolites in the separated fractions (Fig. 5c): such evidences may suggest generally low reactivity levels of the binding material due to unbalanced proportions between lime and pozzolanic additions in the adopted mix design. The low calcium amounts in the binding matrix and the lack of reaction features in the pumice shards, as determined by SEM-EDS (Fig. 5f), constitute a further confirmation of such hypothesis.

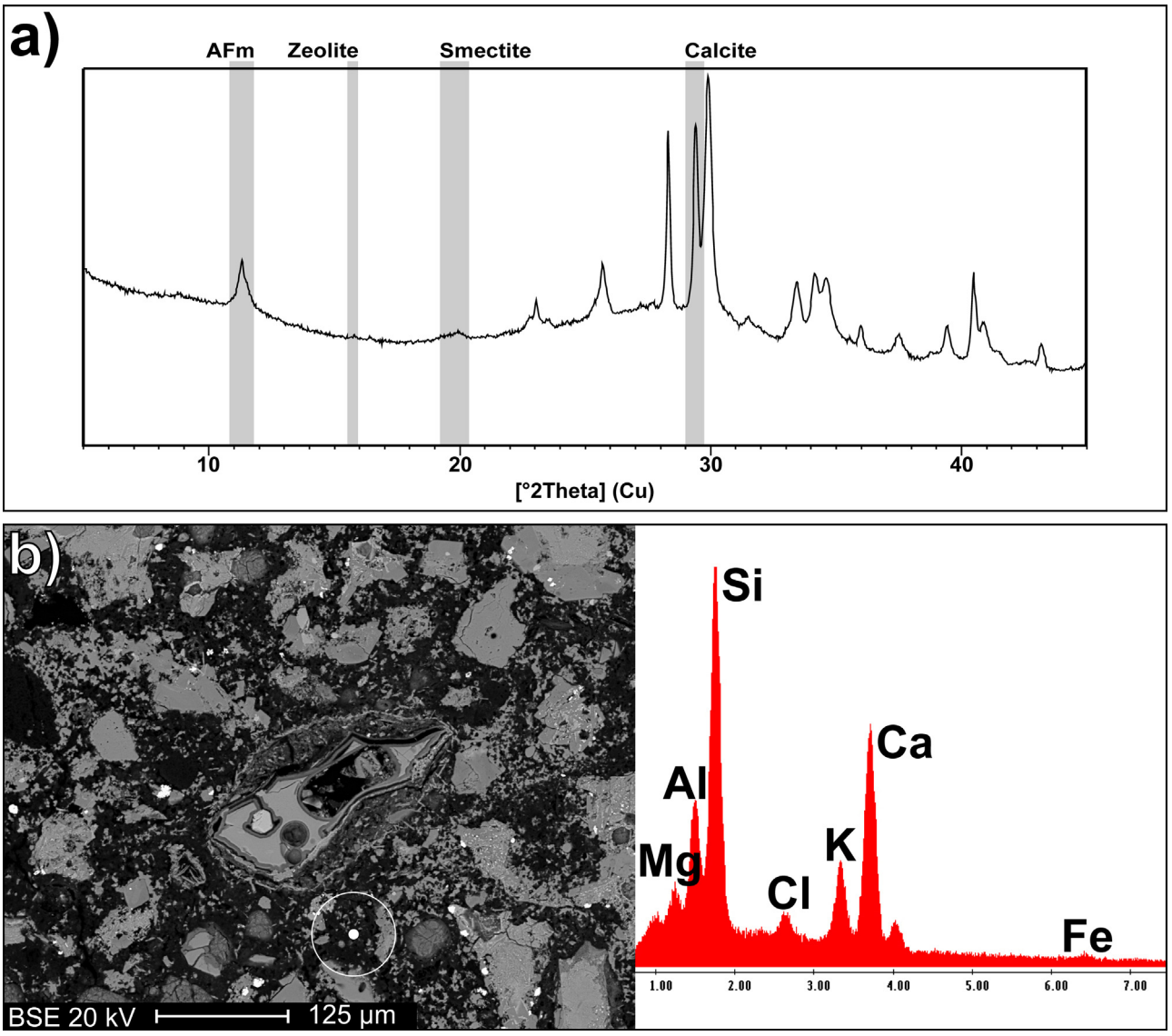

Fig. 6. Mineralogical properties of the binding matrices of group 3 mortars; a: Sample M212, XRPD analysis of the binder fraction; b: Sample M212 BSI and EDS microanalysis of the binder matrix.

Finally, the samples of group 3 are characterized by a relevant occurrence of crystalline carbonate-AFm phase in the binding matrices, associated with calcite formed after partial carbonation of the lime binder (Fig. 6a), indicating a high degree of pozzolanic reactivity of the tephritic foam lava powder employed as aggregate. This is fully confirmed by microchemical analyses (Fig. 6b), showing high silica and alumina concentrations on the matrices and relevant dissolution features on the glassy fraction of the pozzolanic particles.

Discussion and conclusions

The definition of chronological constraints on representative samples of each mineralogical group allowed to interpret the heterogeneous distribution of the binding materials in terms of architectural development of the building over time. More in detail, sample M159 from group 1 has been taken from a partition wall of the *calidarium* surely related to recent restoration interventions, as confirmed by the thermoluminescence dating of one of the bricks constituting the sole masonry unit typology of the structural element. On the other hand, sample M290 of group 2, taken from a portion of wall collapsed from level -3 and unearthed during the archaeological excavation in the area in front of the southern façade [16], can be surely considered as a reference binding material for the main early Imperial construction phase, before the 63 AD earthquake.

Reinterpreting the spatial distribution of the samples in this perspective (Fig. 2a, 2b, 2c), it is clearly observable a preferential concentration of the restoration materials in the uppermost preserved level of the façade and in correspondence of the majority of the vaults and the internal partition walls, while the lower level of the façade, the foundational layers and the perimeter walls are still maintaining the original structural mortars. The distribution of the restoration interventions deduced from the analysis of the mortars allows to chronologically constrain them to the first phases of excavation of the building, under the direction of Antonio Sogliano and August Mau [10], and confirm that at that time only the upper part of the façade was unearthed and restored, while its lower part was still externally covered by debris. Furthermore, the extensive occurrence of restoration materials in the horizontal structural elements and in the partition walls indicates a widespread poor conservation state of the internal part of structure before the 19th century

studies. Such hypothesis finds confirmations in the written works of Mau, referring to massive structural interventions in the rooms of levels −3 and −4 propaedeutic to the execution of the archaeological excavation [12].

Concerning the cement-containing sample (M150) and the materials of group 4, their relation to more recent restoration interventions is corroborated by the position in relation to group 1 samples and by the nature of the structural element of pertinence (e.g. internal walls and vaults).

Finally, group 3 materials can be considered as reference mortars for the first construction phase of the complex, owing their location in proximity to the NW perimeter wall, recognized by Ioppolo as a remnant of the foundational wall sustaining the upper Republican *domus* [11]. The chronological collocation of such structural element and their binding constituents finds a further confirmation considering the widespread utilization of the local tephritic foam lava as construction material in Pompeii during Republican times and especially in the lower parts of the walls [30], as observed also in the southern façade of the Sarno Baths [31].

Apart from the recognition of the different construction phases, crucial technological details on the construction materials employed over time can be determined through the analyses of the binding matrices. Concerning the restoration materials, the utilization of local volcanic sand with high crystalline fraction and low pozzolanic activity indicates the intentional formulation of mix designs aimed at promoting pure aerial reaction processes by lime carbonation. The only exception is related to the structural mortars used for the restoration of the vaults sustaining the *calidarium*, where the utilization of fine volcanic ashes accurately intermixed with the lime binder promoted massive pozzolanic reaction processes. Such technological choice may be aimed at guaranteeing higher structural performances to the related masonry element, given the importance and the large dimensional span of the uppermost room.

On the other hand, the original binding materials are characterized by the utilization of poorly crystalline aggregate fractions rich in fine volcanic ashes and characterized by relevant pozzolanic reactivity, which allowed to shift the reaction path of the binding matrices towards the formation of insoluble Ca-based hydrous compounds characterized by higher mechanical performances and durability with respect to standard aerial binders [32]. It is interesting to note that the utilization of such hydraulic materials is attested in the Sarno Bath complex since Republican times, exploiting the properties of local reactive materials like the Pompeian tephritic foam lava instead of the Phlegrean pyroclastites suggested by Vitruvius in his *De Architectura* [30], which were employed in the subsequent early Imperial construction phase.

Furthermore, the mineralogical characteristics of the early Imperial binding materials gave information on the architectural optimization of the mix designs and on the crucial role of the constituents proportions in the triggering of the binder reaction processes. Firstly, the statistical analysis of the quantitative mineralogical profiles indicated the adoption of higher binder to aggregate ratios for the mortars of the lower −4 level. This can be interpreted as a structural solution employed by Roman masons to increase the load-bearing capacity of complex multi-story buildings like the one analyzed, in accordance with the widely attested Roman tendency to variate the composition of masonry along the height of buildings (as regards Pompeii, see [30]) and in particular to gradate the density of the concrete by employing lightweight aggregates in the upper parts of constructions, as observed in the Pantheon [33] and in many other Roman monuments [34,35]. This information is also consistent with the structural analysis of the building [36,37].

On the other hand, the heterogeneous reaction paths observed in the analyzed mortars can be interpreted in the framework of the competition between carbonation and hydration in lime-pozzolan binding systems. The reaction kinetics is strongly influenced by the solubility properties of reactants, especially pozzolan, by environmental factors, mainly CO_2 partial pressure and moisture content, and by synergic effects between the different influencing factors [38]. Such parameters have little or no influence in case of high reactivity of the pozzolanic material [39], as observed in the present study for the Republican mortars with highly amorphous tephritic foam lava, while their influence is more pronounced for heterogeneous pozzolanic materials like the Phlegrean pyroclastites employed in the Imperial construction phase. At equal proportions and nature of the constituents, the local availability of CO_2 and the water saturation conditions critically control the reaction kinetics. In this perspective, local variations in environmental conditions may have influenced the progression of the reaction processes in the different areas of the analyzed building. However the major factor is the high heterogeneity of the mix proportions observed in the Imperial mortars, especially regarding the amount of added lime, favoring carbonation at increasing values in pozzolanic and geopolymeric systems [40].

Authors contribution

MS, CP and AA designed research; GA and JB supervised the research project; MS, CP, AA, SD and CC performed the samplings; GZ and AK performed the samples preparation; MS, AA and AK analyzed the samples; MS and AA performed the data processing and interpretation; CP performed the architectural analysis and definition of the building phases; all the authors contributed in the writing of the manuscript.

Acknowledgments

The project was carried out in the frame of the Strategic action M̈ultidisciplinary methodological Approaches to the knowledge, conservation and valorization of Cultural Heritage: application to archeological sites(̈MACH) (project: STPD11B3LB_002) supported by University of Padova. Francesca Andolfo is gratefully acknowledged for revising the English text.

Appendix A. Supplementary data

Supplementary material related to this article can be found, in the online version, at https://doi.org/10.1016/j.culher.2019.04.016

References

[1] G. Artioli, M. Secco, A. Addis, The Vitruvian legacy: mortars and binders before and after the Roman world, in EMU Notes in Mineralogy, Contrib. Mineral. Cult. Herit. Eur. Mineral. Union (2019) [In Press].
[2] A. Moropoulou, A. Bakolas, K. Bisbikou, Investigation of the technology of historic mortars, J. Cult. Herit. 1 (1) (2000) 45–58.
[3] F. Carò, M.P. Riccardi, M.T. Mazzilli Savini, Characterization of plasters and mortars as a tool in archaeological studies: the case of Lardirago castle in Pavia, northern Italy, Archaeometry 50 (1) (2008) 85–100.
[4] L.A. Ortega, M.C. Zuluaga, A. Alonso-Olazabal, M. Insausti, A. Ibáñez, Geochemical characterization of archaeological lime mortars: provenance inputs, Archaeometry 50 (3) (2008) 387–408.
[5] D. Miriello, D. Barca, A. Bloise, A. Ciarallo, G.M. Crisci, T. De Rose, C. Gattuso, F. Gazineo, M.F. La Russa, Characterisation of archaeological mortars from Pompeii (Campania, Italy) and identification of construction phases by compositional data analysis, J. Archaeol. Sci. 37 (9) (2010) 2207–2223.
[6] E. Gliozzo, M.C. Dalconi, G. Cruciani, I. Turbanti Memmi, Application of the Rietveld method for the investigation of mortars: a case study on the archaeological site of Thamusida, Eur. J. Mineral. 21 (2) (2009) 457–465.
[7] M.D. Jackson, S.R. Chae, S.R. Mulcahy, C. Meral, R. Taylor, P. Li, A.H. Emwas, J. Moon, S. Yoon, G. Vola, H.R. Wenk, P.J.M. Monteiro, Unlocking the secrets of Al-tobermorite in Roman seawater concrete, Am. Mineral. 98 (10) (2013) 1669–1687.

[8] R. Piovesan, M.C. Dalconi, L. Maritan, C. Mazzoli, X-ray powder diffraction clustering and quantitative phase analysis on historic mortars, Eur. J. Mineral. 25 (2) (2013) 165–175.
[9] F. Noack, K. Lehmann-Hartleben, Baugeschichtliche Untersuchungen and Stradtrand von Pompeji, Walter de Gruyter and Co., Berlin und Leipzig, 1936.
[10] A. Kolowski Ostrow, The Sarno Bath Complex, Roma: «L'Erma» di Bretschneider (1990).
[10] A. Kolowski Ostrow, in: The Sarno Bath Complex, «L'Erma» di Bretschneider, Roma, 1990.
[11] G. Ioppolo, Le Terme del Sarno a Pompei, in: Iter di un'analisi per la conoscenza, il restauro e la protezione sismica del monumento, «L'Erma» di Bretschneider, Roma, 1992.
[12] A. Mau, Scavi di Pompei 1888–1890, Mitt. Dtsch. Archäol. Inst. Römische Abteilung 5 (1890) 111–141.
[13] L. Bernardi, M.S. Busana, The Sarno Baths in Pompeii: context and state of the art, J. Cult. Herit., DOI: 10.1016/j.culher.2019.04.012.
[14] M.S. Busana, L. Bernardi, V. Centola, C. Marson, L. Sbrogiò, The Sarno Baths, Pompeii: architecture development and 3D reconstruction, J. Cult. Herit., DOI: 10.1016/j.culher.2019.04.011.
[15] M. Secco, S. Dilaria, A. Addis, J. Bonetto, G. Artioli, M. Salvadori, The Evolution of the Vitruvian Recipes over 500 Years of Floor-Making Techniques: The Case Studies of the Domus delle Bestie Ferite and the Domus di Tito Macro (Aquileia, Italy), Archaeometry 60 (2) (2018) 185–206.
[16] G. Furlan, J. Bonetto and C. Nicosia, The excavation of the sequence preserved in front of the façade of the Sarno Baths, *J. Cult. Herit.*, DOI: 10.1016/j.culher.2019.04.019.
[17] A. Addis, M. Secco, F. Marzaioli, G. Artioli, A. Chavarria Arnau, I. Passariello, F. Terrasi, G.P. Brogiolo, Selecting the most reliable 14C dating material inside the mortars: the origin of the Padua cathedral, Radiocarbon (2019) 375–393 [In press].
[18] H. Rietveld, A profile refinement method for nuclear and magnetic structures, J. Appl. Crystallography 2 (1969) 65–71.
[19] W. Dollase, Correction of intensities for preferred orientation in powder diffractometry: application of the March model, J. Appl. Crystallography 19 (1986) 267–272.
[20] R. Polino, P. Messina, Carta Geologica d'Italia alla Scala 1:50000, Foglio 466-485 Sorrento-Termini, Napoli, Regione Campania, Settore Geotecnica, Geotermia e Difesa del Suolo, Napoli, 2015.
[21] R. Snellings, G. Mertens, J. Elsen, Supplementary cementitious materials, reviews in mineralogy and geochemistry, Appl. Mineral. Cement Concrete 74 (1) (2012) 211–278.
[22] R. Piovesan, E. Curti, C. Grifa, L. Maritan, C. Mazzoli, Ancient plaster technology: Petrographic and microstratigraphic analysis of plaster-based building materials from the Temple of Venus, Pompeii, in: Interpreting Silent Artefacts: Petrographic Approaches to Archaeological Ceramics, Archaeopress, Oxford, 2009, pp. 65–79.
[23] F. Massazza, Properties and applications of natural pozzolanas, in: Structure and Performance of Cements, Spon Press, London, 2002, pp. 326–352.
[24] T. Matschei, B. Lothenbach, F.P. Glasser, The AFm phase in Portland cement, Cement Concrete Res. 37 (2007) 118–130.
[25] M. Jackson, Sea-Water Concretes and their Material Characteristics, in: Building for Eternity, Oxbow Books, Oxford, 2014, pp. 141–187.
[26] H.F.W. Taylor, Cement Chemistry, Second Edition, Thomas Telford Publishing, London, 1997.
[27] J.M. Melander, L.R. Lauersdorf, Masonry: Design and Construction, Problems and Repair, ASTM, Philadelphia, 1993.
[28] R. Piovesan, Archaeometrical investigations on mortars and paintings at Pompeii and experiments for the determination of the painting technique, University of Padova, PhD Dissertation, Padova, 2009.
[29] M. de'Gennaro, P. Cappelletti, A. Langella, Yellow Tuff: geological, volcanological and mineralogical evidence, Contrib. Mineral. Petrol. 139 (1) (2000) 17–35.
[30] H. Dessales, Les savoir-faire des maçons romains, entre connaissance technique et disponibilité des matériaux. Le cas pompéien, in: N. Monteix, N. Tran (Eds.), Les savoirs professionnels des gens de métier. Études sur le monde du travail dans les sociétés urbaines de l'empire romain, Centre Jean Bérard, Naples, 2011, pp. 41–63.
[31] R. Piovesan, L. Maritan, G. Meneghin, C. Previato, S. Baklouti, R. Sassi and C. Mazzoli, Stones of the façade of the Sarno Baths, Pompeii: a mindful construction choice, *J. Cult. Herit.*, DOI: 10.1016/j.culher.2019.04.010.
[32] M.D. Jackson, E.N. Landis, P.F. Brune, M. Vitti, H. Chen, Q. Li, M. Kunz, H.R. Wenk, P.J.M. Monteiro, AR. Ingraffea, Mechanical resilience and cementitious processes in Imperial Roman architectural mortar, Proc. Nat. Acad. Sci. 111 (52) (2014) 18484–18489.
[33] R. Mark, P. Hutchinson, On the Structure of the Roman Pantheon, Art Bull. 68 (1) (1986) 24–34.
[34] L.C. Lancaster, Concrete Vaulted Construction in Imperial Rome. Innovations in context, Cambridge University Press, Cambridge, 2005.
[35] L.C. Lancaster, Innovative Vaulting in the architecture of the Roman Empire. 1st to 4th centuries CE, Cambridge University Press, New York, 2015.
[36] M.R. Valluzzi, F. Lorenzoni, R. Deiana, S. Taffarel, C. Modena, Non-destructive investigations for structural qualification of the Sarno Baths, Pompeii, *J. Cult. Herit.*, DOI: 10.1016/j.culher.2019.04.015.
[37] F. Lorenzoni, M.R. Valluzzi, C. Modena, Seismic assessment and numerical modelling of the Sarno Baths, Pompeii, J. Cult. Herit., DOI: 10.1016/j.culher.2019.04.017.
[38] Ö. Cizer, Competition between carbonation and hydration on the hardening of calcium hydroxide and calcium silicate binders, K.U. Leuven, PhD dissertation, Leuven, 2009.
[39] Ö. Cizer, K. Van Balen, D. Van Gemert, Competition between hydration and carbonation in hydraulic lime and lime-Pozzolana mortars, Adv. Mater. Res. 133-134 (2010) 241–246.
[40] G. Arcones-Pascual, F. Hernández-Olivares, A. Sepulcre-Aguilar, Comparative properties of a lime mortar with different metakaolin and natron additions, Construct. Build. Mater. 114 (2016) 747–754.
[41] M. Monego, A. Menin, M. Fabris and V. Achilli, 3D survey of Sarno Baths (Pompeii) by integrated geomatic methodologies, *J. Cult. Herit.*, DOI: 10.1016/j.culher.2019.04.013.